Electronic Supporting Information

Caught! Crystal Trapping of a side-on peroxo bound to Cr(IV)

David P. de Sousa,[a] Jennifer Bigelow,[b] Jonas Sundberg,[a] Lawrence Que Jr.[b] and Christine J. McKenzie*[a]

[a] *Department of Physics, Chemistry and Pharmacy, University of Southern Denmark, Campusvej 55, 5230 Odense M (Denmark). Fax: +45 6615 8760; Tel: +45 6550 2518; E-mail: mckenzie@sdu.dk*
[b] *Department of Chemistry and Center for Metals in Biocatalysis, University of Minnesota, Minneapolis, Minnesota, 55455, USA*

Supporting figures and tables

Experimental Details

Elemental analysis was performed at the Chemistry Department at Copenhagen University. ATR-IR spectra were recorded as neat solids on a PerkinElmer Spectrum Two spectrometer. All spectra have been ATR- and baseline corrected. UV-Vis spectra were recorded on an Agilent 8453 spectrophotometer using 1 cm quartz cuvettes. EPR spectra where recorded on a Bruker EMX Plus CW spectrometer. ESI-MS spectra were recorded on a microspray LC-MS Bruker micrOTOF-Q II spectrometer. CV spectra were recorded using an Autolab system controlled by the GPES software. The working electrode was a platinum disk, the auxiliary electrode a platinum wire and the reference electrode an Ag wire/Ag^+ (10 mM $AgNO_3$). Electrodes were polished with diamond paste, rinsed and sonicated before use. Resonance Raman spectra where collected using Spectra-Physics Model 2060 Kr^+ and 2030-15 Ar^+ lasers and an Action AM-506 monochromator equipped with a Princeton LN/CCD data collection system. Samples were generated and then frozen in EPR tubes in liquid nitrogen. Spectra were obtained at 77 K and kept cold with liquid nitrogen in an EPR dewar. Raman frequencies were calibrated to indene prior to data collection. The monochromator slit width was set for a bandpass of 4 cm^{-1} for all spectra. X-ray crystal diffraction data were collected using a Bruker-Nonius X8 APEX-II instrument (Mo-Kα radiation, graphite monochromated fine-focused sealed tube). Structure solution was carried out with SHELXS-2013, and refined against F^2 by full matrix least squares using SHELXL-2013. Hydrogen atoms was placed at calculated positions and allowed to ride on their carrier atoms with isotropic displacement parameters $U_{iso}(H) = 1.2U_{eq}$. **Syntheses.** Commercially available reagents were purchased from Sigma-Aldrich and used without further purification. $Na_2(tpena)_2(CH_3CH_2OH)_2$ was synthesized following Vad *et al.*[1]. Acetonitrile and diethylether were dried over activated 3 Å mol sieves and contain 10 and 9 ppm residual water, respectively, as measured by Carl-Fisher titration.
Caution: Perchlorate salts are potentially explosive upon exposure to excess heat or shock, and should be handled with care and only in small quantities.

$[Cr(tpena)](ClO_4)_2(C_4H_8O_2)_{0.5}$. ($1.(ClO_4)_2(C_4H_8O_2)_{0.5}$). 111 mg (0.12 mmol) $Na_2(tpena)_2(CH_3CH_2OH)_2$ was dissolved in 1 mL water. A filtered solution of 96 mg (0.24 mmol) $Cr(NO_3)_6{\cdot}9H_2O$ and 68 mg (0.48 mmol) $NaClO_4{\cdot}H_2O$ in 1 mL water was added. The solution was acidified with 1 drop of 12 M perchloric acid. Initially a thick blue-green dispersion was formed, but after stirring for 1 hr at rt, the solution became almost clear red. The solution was diluted with 3 mL dioxane and filtered. Slow evaporation of the filtered solution yielded the product as red rubies over 10 days (102 mg, 62%). Anal. Calc. for $C_{24}H_{28}Cl_2CrN_5O_{11}$: C, 42.06; H, 4.12; N, 10.22. Found: C, 41.95; H, 3.97; N, 10.08. ESI-MS (H_2O), *m/z*: 442.1 ($[Cr^{II}(tpena)]^+$, 17%), 459.1 ($[Cr^{III}(tpena)OH]^+$, 100%). IR (neat): 1681 (vs, br, C=O), 1611 (s), 1336 (m), 1298 (br, s, C=O), 1091 (vs, br, ClO_4), 1031 (m), 772 (s, br, ClO_4), 624 cm^{-1} (s). UV-Vis (H_2O): 366 (86), 483 nm (139 $M^{-1}cm^{-1}$); UV-Vis (CH_3CN): 376 (104), 487 nm (189 $M^{-1}cm^{-1}$).

(1) M. S. Vad, A. Nielsen, A. Lennartson, A. D. Bond, J. E. McGrady, C. J. McKenzie, *Dalton Trans.*, 2011, **40**, 10698.

$[CrO_2(tpenaH)](ClO_4)_2$ (4.(ClO_4)). 40 mg (58 µmol) $[Cr^{III}(tpena)](ClO_4)_2(C_4H_8O_2)_{0.5}$ was dissolved in 3 mL acetonitrile and added 3 ml (32 mmol) 10.9 M H_2O_2 (*aq*). After stirring for 40 mins a dark violet powder was precipitated by addition of 12 mL 3:2 diethylether/dioxane and isolated by centrifugation. The solid was dried over a stream of nitrogen and stored at -40 °C (25 mg, 64%). X-ray grade crystals of were grown by placing two large single crystals of **1**.$ClO_4)_2(C_4H_8O_2)_{0.5}$ in a drop of 33% H_2O_2 (*aq*) in a covered glass container. After standing undisturbed at 4 °C for ~24 hs violet plates of **4**.$(ClO_4)_2(H_2O_2)_4$ formed. ESI-MS (H_2O), *m/z*: 350.10 ($[Cr^{III}(tpena \div CHC_5H_4N)]^+$, 6%), 442.1 ($[Cr^{II}(tpena)]^+$, 100%), 459.1 ($[Cr(tpena)OH)]^+$, 14%), 474.1 ($[CrO_2(tpena)]^+$, 34%). IR (neat): 1669 (vs, br, C=O), 1608 (s), 1373 (m), 1256 (br, s, C=O), 1095 (vs, br, ClO_4), 890 (m), 871 (vs, s, O-O), 624 cm^{-1} (s). UV-Vis (H_2O): 535 nm (142 $M^{-1}cm^{-1}$); UV-Vis (CH_3CN): 553 nm (150 $M^{-1}cm^{-1}$).

Generation of $[Cr(tpena)OH]^+$ (3). If solutions of $[Cr(tpena)]^{2+}$ (**1**) in water or acetonitrile are made alkaline with NaOH or Et_3N, the "true" hydroxide $[Cr(tpena)OH]^+$ (**3**) is formed. The formation of **3** is indicated by a color change from red to blue (UV-Vis (H_2O) = 410, 561 nm (63, 88 $M^{-1}cm^{-1}$); UV-Vis (CH_3CN) = 409, 578 nm (112, 137 $M^{-1}cm^{-1}$)). The blue solutions of **3** also yields aqueous ESI-MS spectra with $[Cr^{III}(tpena)OH]^+$ as the dominant ion. The conversion is accompanied by a dramatic change in electrochemical behaviour. In contrast to $[Cr(tpena)]^{2+}$, only irreversible aqueous electrochemistry is observed for **3**, with an strong irreversible oxidation peak in the anodic region, E_{pa} = + 571 mV (*vs* Ag/Ag^+; $Cr^{III}OH/Cr^{IV}OH$), and a irreversible reduction peak in the catodic region at E_{pc} = - 830 mV ($Cr^{III}OH/Cr^{II}OH$).

Bond Valence Analysis

The BVS analysis was carried out as previously reported[2,3] using the formula $BVS = \sum_i [r_0(M\text{-}X) - r_i(M\text{-}X)] / 0.73$ Å and $r_0(M\text{-}O) = 1.759$ Å, $r_0(M\text{-}N) = 1.831$ Å. For reference a BVS = 3.306 was obtained for $[Cr^{III}(tpena)](ClO_4)_2$. The published structure of $[Cr^{IV}O_2(TMC)OH_2]Cl_2$ yielded a BVS = 3.635. The validity of the model was confirmed by calculating the BVS of 15 known mononuclear Cr(IV) compounds from the Cambridge Structural Database (2014) with O and N donors, which yielded an average BVS = 4.039 ± 0.366.

(2) F. B. Larsen, A. Boisen, K. J. Berry, B. Moubaraki, K. S. Murray, V. McKee, R. C. Scarrow, C. J. McKenzie, *Eur. J. Inorg. Chem.*, 2006, 3841;

(3) L. Shu, Y.-M. Chiou, A. M. Orville, M. A. Miller, J. D. Lipscomb, L. Que Jr., *Biochemistry (Mosc.)*, 1995, **34**, 6649.

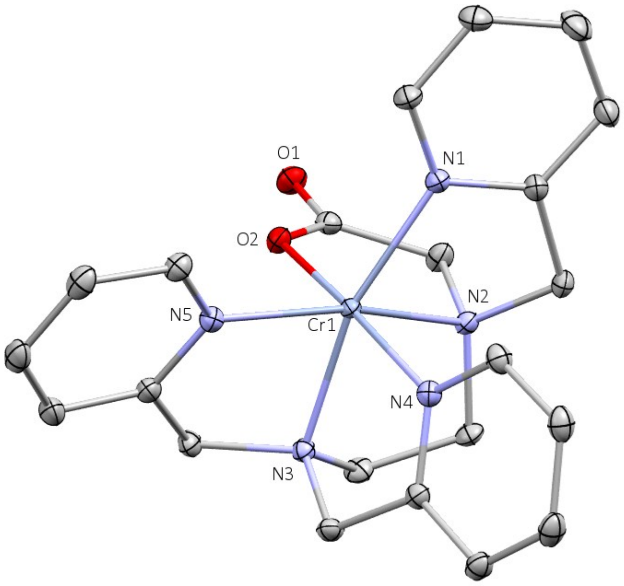

Figure S1. ORTEP plot of the cation, **1**, of [Cr(tpena)]$(ClO_4)_2(C_4H_8O_2)_{0.5}$ showing 50% probability ellipsoids. See Table S3 for selected bond distances and angles.

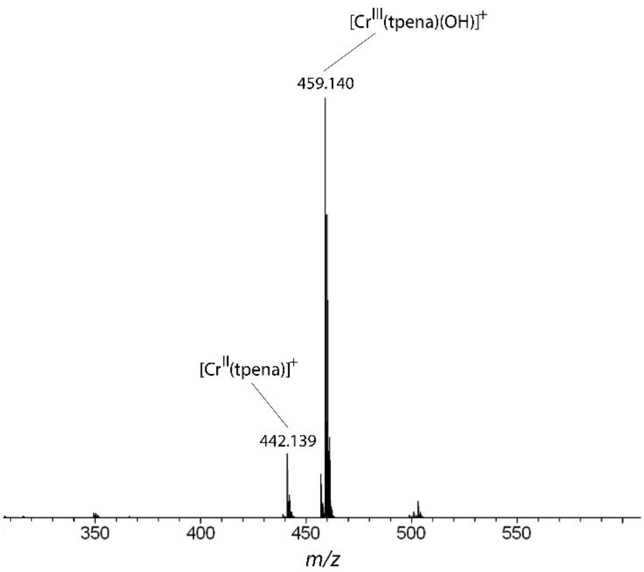

Figure S2. ESI-MS spectra of [Cr(tpena)]$(ClO_4)_2(C_4H_8O_2)_{0.5}$ dissolved in H_2O.

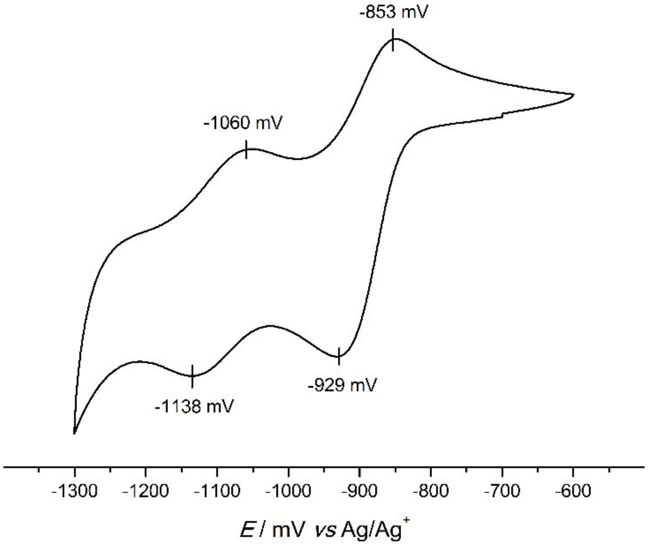

Figure S3. CV of 1 mM [Cr(tpena)]$(ClO_4)_2$ dissolved in 0.1 M aqueous KPF_6. The redox couple at $E_{½}$ = - 1099 (*vs* Ag/Ag^+) is assigned to $[Cr^{III}(tpena)]^{2+}/[Cr^{II}(tpena)]^+$. The redox couple at $E_{½}$ = - 885 mV is assigned to $[Cr^{III}(tpena)OH_2]^{2+}/[Cr^{II}(tpena)OH_2]^+$. Sweep rate: 10 mV s^{-1}.

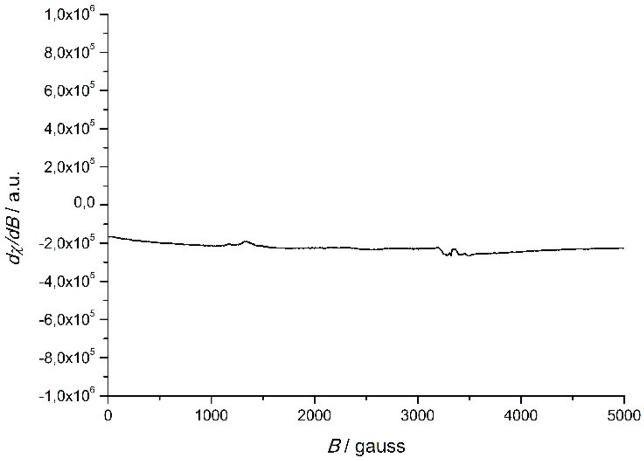

Figure S4. X-band EPR spectrum of a frozen 5 mM CH_3CN solution of $[CrO_2(tpenaH)]^{2+}$ at 110 K.

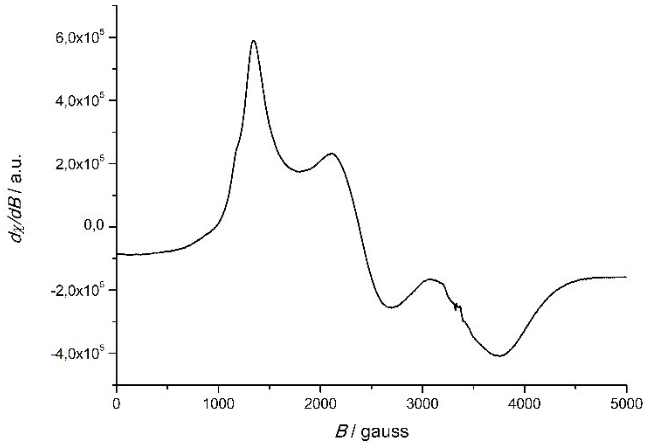

Figure S5. X-band EPR spectrum of a frozen 5 mM CH_3CN solution of $[Cr(tpena)]^{2+}$ at 110 K.

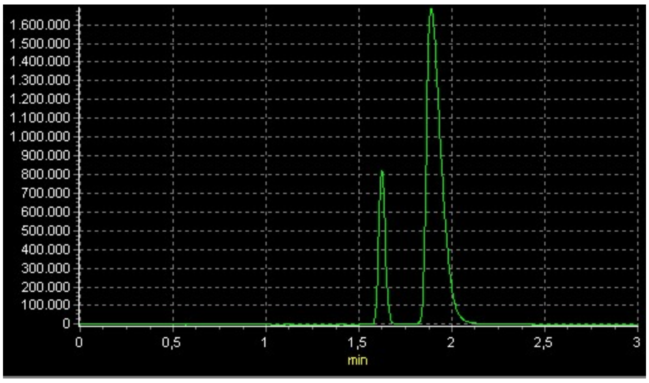

Figure S6. GC-TCD chromatogram of the headspace gas of the reaction of $[Cr(tpena)]^{2+}$ with excess H_2O_2. The reaction were carried out under an initially oxygen free N_2 atmosphere. The signal at 1.62 min is due to O_2 and the signal at 1.90 min is due to N_2.

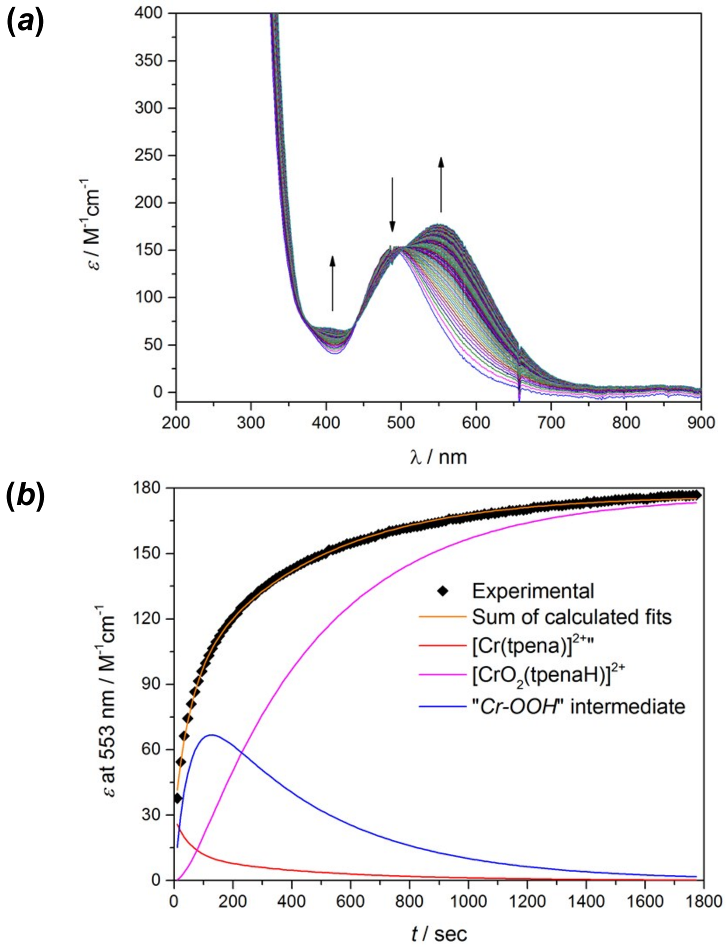

Figure S7. (*a*) Time resolved UV-Vis spectra of the oxidation of a 2 mM CH_3CN solution of $[Cr(tpena)]^{2+}$ after addition of 700 eq. 11.9 M aqueous H_2O_2 (1.26 M). (***b***) Numerical fitting and simulation of the speciation for the kinetic trace at λ = 553 nm with Reactlab KINSIM.

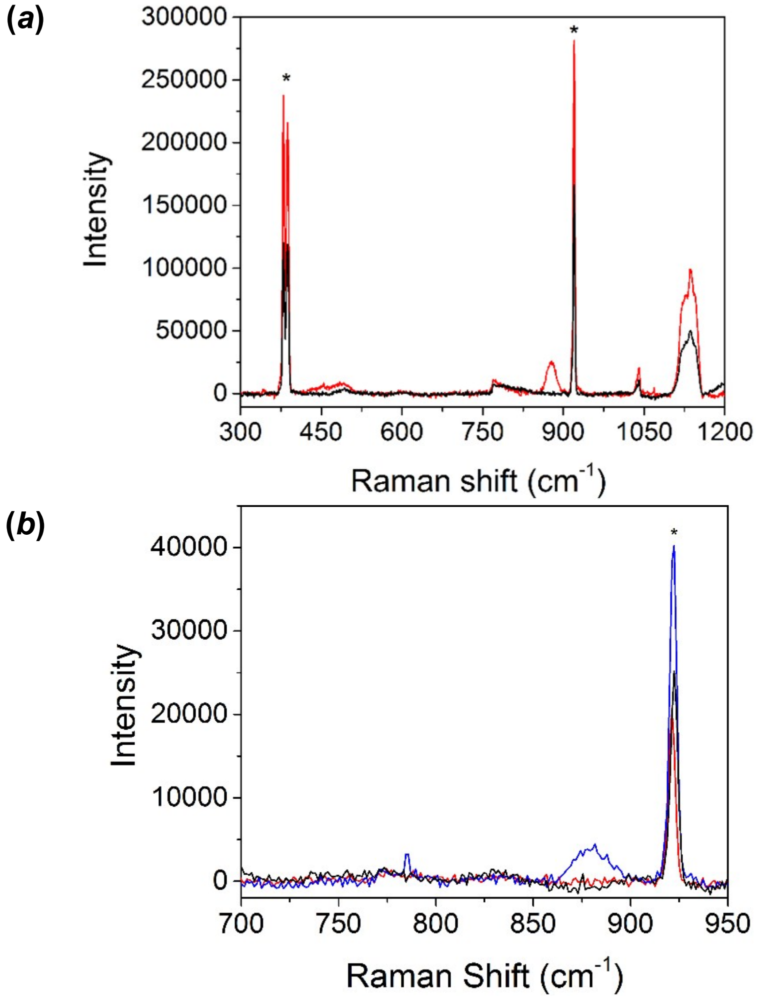

Figure S8. Frozen solution resonance Raman spectra. (***a***) Full range of spectrum from main article (***b***) Spectrum recorded with an excitation wavelength of $\lambda_{ex} = 413.1$.nm (power = 65 mW). $[CrO_2(tpenaH)]^{2+}$ (blue line, 7.9 mM, generated *in-situ* from $[Cr(tpena)]^{2+}$ and 200 eq 30% H_2O_2) in CH_3CN, 9 mM $[Cr(tpena)]^{2+}$ (red line, 9 mM) in CH_3CN, $[Cr(tpena)OH]^{+}$ (black line, 9 mM, generated *in-situ* from $[Cr(tpena)]^{2+}$ and 1.2 eq Et_3N) in 9:1 CH_3CN/H_2O.

Table S1. Stretching vibrations of Cr-OO complexes.

Complex	v(O-O) / cm^{-1}	Ref.
"end-on" superoxo		
$[Cr^{III}(OO)(OH_2)_6]^+$	1166	Bakac *et al.*[4]
$[Cr^{III}(OO)(cyclam)(H_2O)]^{2+}$	1134/1145	Bakac *et al.*[4]
$[Cr^{III}(OO)(14\text{-}TMC)(Cl)]^+$	1170	Cho *et al.*[5]
"side-on" superoxo		
$[Cr^{III}(O_2)(Tp^{tBu,Me})(C_6H_5N)]^+$	1083	Qin *et al.*[6]
"side-on" peroxo		
$[Cr^{V}(O_2)_4]^{3-}$	875	Fergussion *et al.*[7]
$[Cr^{IV}(O_2)(12\text{-}TMC)(Cl)]^+$	864	Yokoyama *et al.*[8]
$[Cr^{IV}(O_2)(tpenaH)]^{2+}$	878	This work

(4) A. Bakac, S. L. Scott, J. H. Espenson, K. R. Rodgers, *J. Am. Chem. Soc.* 1995, **117**, 6483.

(5) J. Cho, J. Woo, W. Nam, *J. Am. Chem. Soc.* 2010, **132**, 5958.

(6) K. Qin, C. D. Incarvito, A. L. Rheingold, K. L. Theopold, *Angew. Chem. Int. Ed.* 2002, **41**, 2333.

(7) J. E. Fergusson, C. J. Wilkins, J. F. Young, *Chem. Soc. Resumed* 1962, 2136.

(8) A. Yokoyama, J. E. Han, J. Cho, M. Kubo, T. Ogura, M. A. Siegler, K. D. Karlin, W. Nam, W. *J. Am. Chem. Soc.* 2012, **134**, 15269.

Crystallographic information for [CrO_2(tpenaH)](ClO_4)$_2$(H_2O_2)$_3$(H_2O).

Table S2. Selected crystallographic data for [CrO_2(tpenaH)](ClO_4)$_2$(H_2O_2)$_3$(H_2O).

Empirical formula	$C_{22}H_{33}Cl_2CrN_5O_{19}$
Formula weight (g/mol)	794.42
Temperature (K)	150
Crystal system	monoclinic
Space group	$P2_1/n$
a, b, c (Å)	15.2360 (16), 14.7664 (16), 16.0081 (17)
α, β, γ (°)	90, 118.237 (5), 90
Volume (Å^3)	3172.9 (6)
Z	4
ρ_{calc} (g cm^{-3})	1.680
Abs. coefficient (mm^{-1})	0.624
F(000)	1640
Crystal size (mm^3)	0.28 x 0.13 x 0.04
2Θ range for data collection	2.5 to 30.6°
Index ranges	$-19 \leq h \leq 19$, $-18 \leq k \leq 18$, $-18 \leq l \leq 20$
Reflections collected	43356
Independent reflns (R_{int})	6434 (0.082)
Data / restraints / parameters	6434 / 1 / 454
GOF on F^2	1.076
Final $R_1(F)^a$ (I > 2σ(I)) / $wR_2(F^2)^b$	0.1053 / 0.2912
$R_1{}^a$ / $wR_2(F^2)^b$ (all data)	0.1325 / 0.3083
Largest diff. peak / hole (eÅ^{-3})	2.26 / -0.77

[a] $R_1(F) = \Sigma(||F_o| - |F_c||) / \Sigma|F_o|$

[b] $wR_2(F^2) = \{\Sigma[w(F_o^2 - F_c^2)^2] / \Sigma [w(F_o^2)^2]\}^{½}$

Table S3. Selected bond distances (Å) and angles (^{o}) for $[\mathrm{CrO_2(tpenaH)}](\mathrm{ClO_4})_2(\mathrm{H_2O_2})_3(\mathrm{H_2O})$

Cr1 – O2	1.931 (5)
Cr1 – O3	1.884 (5)
Cr1 – O4	1.884 (5)
Cr1 – N4	2.041 (6)
Cr1 – N5	2.086 (6)
Cr1 – N3	2.109 (6)
Cr1 – N2	2.165 (6)
O4 – O3	1.383 (8)
O3 – Cr1 – O4	43.1 (2)
O3 – O4 – Cr1	68.5 (2)
O4 – O3 – Cr1	68.5 (3)
O3 – Cr1 – O2	95.3 (2)
O4 – Cr1 – O2	94.4 (2)
Cr1 – N2 – C6	113.4 (4)
N2 – Cr1 – O3	79.5 (2)
N2 – Cr1 – O4	122.2 (2)
N2 – Cr1 – N3	81.2 (2)
N2 – Cr1 – N4	92.5 (2)
N2 – Cr1 – N5	155.1 (2)
N2 – Cr1 – O2	82.9 (2)
N3 – Cr1 – O3	159.9 (2)
N3 – Cr1 – O4	156.5 (3)
N3 – Cr1 – N4	81.8 (2)
N3 – Cr1 – N5	75.5 (2)
N3 – Cr1 – O2	88.2 (2)
N4 – Cr1 – O3	124.3 (2)
N4 – Cr1 – O4	95.9 (3)
N4 – Cr1 – N5	93.1 (2)
N4 – Cr1 – O2	169.6 (2)
N5 – Cr1 – O3	124.3 (2)
N5 – Cr1 – O4	81.3 (3)
N5 – Cr1 – O2	87.3 (2)

Crystallographic information for $[Cr(tpena)](ClO_4)_2(C_6H_8O_2)_{0.5}$

Table S4. Selected crystallographic data for $[Cr(tpena)](ClO_4)_2(C_4H_8O_2)_{0.5}$.

Empirical formula	$C_{24}H_{28}Cl_2CrN_5O_{11}$
Formula weight (g/mol)	685.41
Temperature (K)	100
Crystal system	monoclinic
Space group	$P2_1/c$
a , b, c (Å)	16.3004 (14), 12.4635 (11), 13.5694 (12)
α, β, γ (°)	90, 91.647 (5), 90
Volume (Å^3)	2755.6 (4)
Z	4
ρ_{calc} (g cm^{-3})	1.652
Abs. coefficient	0.680
F(000)	1412.0
Crystal size (mm^3)	0.50 x 0.28 x 0.20
2Θ range for data collection	4.114 to 61.412°
Index ranges	$-23 \leq h \leq 23$, $-17 \leq k \leq 17$, $-19 \leq l \leq 19$
Reflections collected	88931
Independent reflns (R_{int})	8510 (0.0321)
Data / restraints / parameters	8510 / 0 / 388
GOF on F^2	1.088
Final $R_1(F)^a$ ($I > 2\sigma(I)$) / $wR_2(F^2)^b$	0.0281 / 0.0796
$R_1{}^a$ / $wR_2(F^2)^b$ (all data)	0.0341 / 0.0878
Largest diff. peak / hole (eÅ^{-3})	0.62 / -0.54

[a] $R_1(F) = \Sigma(||F_o| - |F_c||)/\Sigma|F_o|$

[b] $wR_2(F^2) = \{\Sigma[w(F_o^2 - F_c^2)^2] / \Sigma [w(F_o^2)^2]\}^{½}$

Table S5. Selected bond distances (Å) and angles (^{o}) for $[Cr(tpena)](ClO_4)_2(C_4H_8O_2)_{0.5}$

Cr1 – N1	2.0590 (11)
Cr1 – N2	2.0631 (10)
Cr1 – N3	2.0516 (10)
Cr1 – N4	2.0651 (10)
Cr1 – N5	2.0717 (11)
Cr1 – O2	1.9310 (9)
N1 – Cr1 – O2	93.43 (4)
N1 – Cr1 – N2	79.64 (4)
N1 – Cr1 – N3	163.57 (4)
N1 – Cr1 – N4	90.60 (4)
N1 – Cr1 – N5	115.40 (4)
N2 – Cr1 – O2	83.88 (4)
N2 – Cr1 – N3	85.69 (4)
N2 – Cr1 – N4	92.54 (4)
N2 – Cr1 – N5	163.58 (4)
N3 – Cr1 – O2	92.31 (4)
N3 – Cr1 – N4	82.64 (4)
N3 – Cr1 – N5	80.11 (4)
N4 – Cr1 – O2	174.03 (4)
N4 – Cr1 – N5	93.78 (4)